SHIRMS 2008 – Y. Potvin, J. Carter, A. Dyskin, R. Jeffrey (eds)

doi:10.36487/ACG_repo/808_58

The Variable Rate of Sand Production Captured by an Analytical Model

E. Fjær *The Foundation for Scientific and Industrial Research (SINTEF) Petroleum Research, and Norwegian University of Science and Technology, Norway*

E. Papamichos *Aristotle University of Thessaloniki, Greece, and The Foundation for Scientific and Industrial Research (SINTEF) Petroleum Research, Norway*

Abstract

An analytical model for the rate of sand production from cylindrical cavities has been calibrated on laboratory tests, and used for prediction of sand production under field-like conditions. The model is based on the assumption that sand production is driven by erosion from plastified material around the cavity. The model predicts, in agreement with field observations, that sand production may occur in different forms: It may be continuous, at a relatively constant rate; it may be transient, where continuous production at a declining rate follows a burst of sand, or it may be catastrophic, where sand is produced at a very high rate. The predictions are found to vary significantly, depending on rock type, in situ *stress and pore pressure conditions, and well pressure and fluid flow rate.*

1 Introduction

Sand produced along with hydrocarbons represents an economical problem as well as a safety risk and an environmental challenge. Since measures to produce sand free hydrocarbons are costly, and often imply reduced productivity, it may be desirable to allow for some sand production and produce under a maximum allowable sand rate criterion (Hettema et al., 2006). The ability to predict the rate of sand production prior to the start of the production, or prior to changes in the production procedures is, however, important for efficient production under such conditions.

Sand production experiments run on outcrop and reservoir cores reveal that the cavity of hollow cylinders fails in three distinct patterns, depending on the sandstone type. The sandstones are classified according to the cavity failure pattern in three classes, Class A – brittle, Class B – ductile, and Class C – compactive (Papamichos et al., 2008). Sand measurement results show that the failure type has a direct consequence on the observed sand rate. Class A shows rapid sand rate increase with increasing stress, Class B shows a slow down period after initial sand production and Class C shows a slow increase of sand rate with increasing stress. The typical failure patterns for the three classes are illustrated in Figure 1.

In Class A, we have the development of slit like breakouts. They seem to start as concave breakouts indicating tensile failure and develop to planar slits (not holes) that run along the whole height of the specimen.

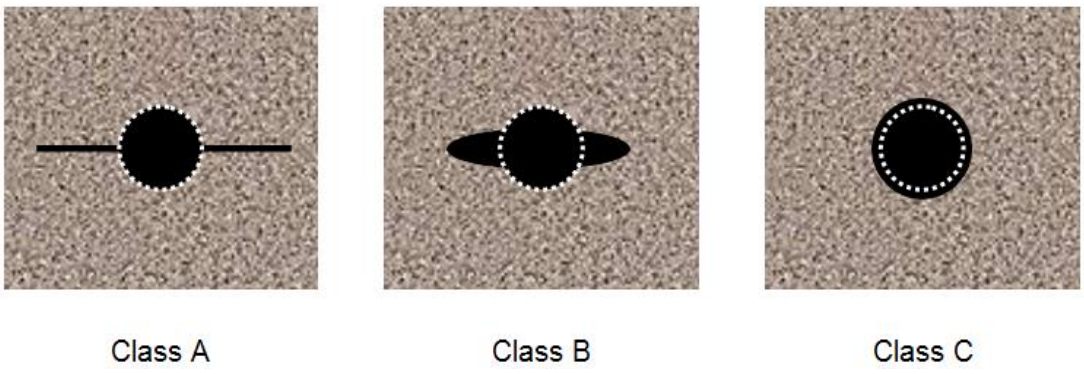

Figure 1 Schematic illustrations of the failure modes typical for the three rock classes. The white dotted lines indicate the initial size and shape of the cavity

In Class B, we have the development of convex breakouts due to shear failure. With increasing confining stress, more shear bands develop and make the breakouts longer. The failed material is often in the form of slabs and may get trapped inside the breakouts and/or the cavity.

In Class C, we have the development of uniform failure around the cavity which is eroded the flowing fluid resulting in a relatively uniform enlargement of the cavity.

A simplified analytical model describing the rate of sand production from a cylindrical cavity has previously been presented (Fjær et al., 2004; 2008). The model is based on the basic principles of the numerical model of Papamichos et al. (2001). The basic features of the model are described in Section 2. Here we shall use modified versions of this model in order to describe the behaviour observed in laboratory tests. Finally, we give some examples of sand rate predictions, using the calibrated versions of the model.

2 The analytical model

Our analytical model describes sand production from a cylindrical cavity. The model is based on the assumption that sand production is an erosion process driven by the fluid flow, so that the rate of sand production is strongly related to the hydrodynamic forces acting on the sand grains. The rock volume from which sand erosion can take place is a thin layer at the cavity wall. The thickness of this layer is controlled by the stress conditions, since damage of the rock is a necessary condition for sand production.

As sand is produced from the damaged layer, the porosity of the layer increases and its ability to carry load is reduced. This erosion-mechanical coupling is accounted for by assuming that the sand producing rock keeps its stiffness despite erosion, until a critical limit is reached where the whole structure collapses. This construction implies that sand is produced in bursts, in accordance with laboratory observations. A derivation of the model is given in Fjær et al. (2008).

According to this model, the rate of sand production, $\dot{M}_{sand}$, can be expressed as:

$$\dot{M}_{sand} = M_{sand}\frac{2}{\tau_s}\frac{D-D_c}{C_0}\left(\frac{Q}{Aq_{fl}^{cr}}-1\right) \tag{1}$$

Where:

D_c = critical drawdown (= drawdown at onset of sand production).

C_0 = unconfined compressive strength.

Q = fluid flow rate.

q_{fl}^{cr} = critical fluid flux for sand erosion (= lower limit for the fluid flux Q/A in order to uphold the erosion process).

τ_s = characteristic sand erosion time.

Further:

$$A = 2\pi R_c L \tag{2}$$

is the inflow area (where R_c is the cavity radius, and L is the cavity length), and

$$M_{sand} = \pi R_c^2 L \rho_s \left(1-\phi_0\right) \tag{3}$$

is the cumulative amount of sand produced from the cavity, including the amount initially removed in order to create the cavity. Here ρ_s is the grain density, and ϕ_0 the initial porosity.

The inverse of the characteristic sand erosion time (that is: $1/\tau_s$) represents the speed of the erosion process. More precisely, the time Δt from the erosion process starts until the sand producing layer collapses is proportional to τ_s and is given as:

$$\Delta t = \tau_s \left(\frac{Q}{A q_{fl}^{cr}} - 1 \right)^{-1} \tag{4}$$

Note that two conditions have to be fulfilled for sand to be produced, according to Equation (1). Firstly, it is required that $D > D_c$, which expresses the fact that stress induced damage of the rock is a necessary condition for sand production. Secondly, it is required that $(Q/A) > q_{fl}^{cr}$, which expresses that the hydrodynamic forces must be strong enough to uphold the erosion process.

Equation (1) is based on the assumption that sand is produced uniformly from the cavity surface, such that the cavity maintains its cylindrical shape while sand is being produced. Also, Equation (1) is based on the assumption that the drawdown D is not much larger than the critical drawdown D_c, such that:

$$e^{(D-D_c)/C_0} - 1 \approx \frac{D - D_c}{C_0} \tag{5}$$

As these assumptions are not always fulfilled, a more general form of the expression for $\dot{M}_{sand}$ will be needed:

$$\dot{M}_{sand} = R_c A_{sp} \rho_s (1 - \phi_0) \frac{1}{\tau_s} \left(e^{(D-D_c)/C_0} - 1 \right) \left(\frac{Q_{sp}}{A_{sp} q_{fl}^{cr}} - 1 \right) \tag{6}$$

Here A_{sp} is the surface area through which sand is being produced, and Q_{sp} is the fluid flow rate through the same area. Note that Equations (1) and (6) represent an average rate, where the small bursts related to the discontinuous breakdown of the failed material have been smoothed out.

The critical drawdown D_c is a function of the rock properties and the in situ stresses and pore pressure. A simple expression that captures these dependencies for a cylindrical cavity in an isotropic stress field is (Fjær et al., 2008):

$$D_c = A_1 \left(C_0 - 2\sigma_h' \right) + A_2 \tag{7}$$

A_1 and A_2 are rock specific constants, while σ_h' is the effective (isotropic) in situ stress. (Fjær et al., 2008) for a discussion of stress anisotropy effects in relation to this expression.

3 Calibration

Here we present the calibration of the model on three rocks. The three rock types have different cavity failure behaviour in sand production tests and thus may be placed in different classes (Papamichos et al., 2008).

3.1 Laboratory tests used for calibration

Laboratory tests in hollow cylinders were used to simulate sand production from cylindrical cavities. The hollow cylinders were about 20 cm long, with 10 cm external radius and 1 cm inner radius (Figure 2). External stress σ_e is provided by a confining oil and pistons at the end surfaces. The cylindrical surface of the sample is shielded from the confining oil by a flexible sleeve. The flowing fluid enters the sample at a pressure p_e through a layer of packed proppant situated between the sample and the sleeve and flows radially towards the inner surface where the pressure is atmospheric. Produced sand is captured by a sand trap and recorded by real time weight measurements. The time lag from when the sand is released from the rock until it reaches the sand trap is estimated to be less than five seconds. The flowing fluid is lamp paraffin, with viscosity 1.4 cP. The external stress σ_e is kept isotropic for all tests. The test procedure has been described in more detail by Papamichos et al. (2001).

During a test, p_e and σ_e can be varied independently, which allows for nearly independent variation of Q and $D - D_c$. The effective in situ stress is estimated to be $\sigma_h' = \sigma_e - p_e$ and the drawdown $D = p_e$.

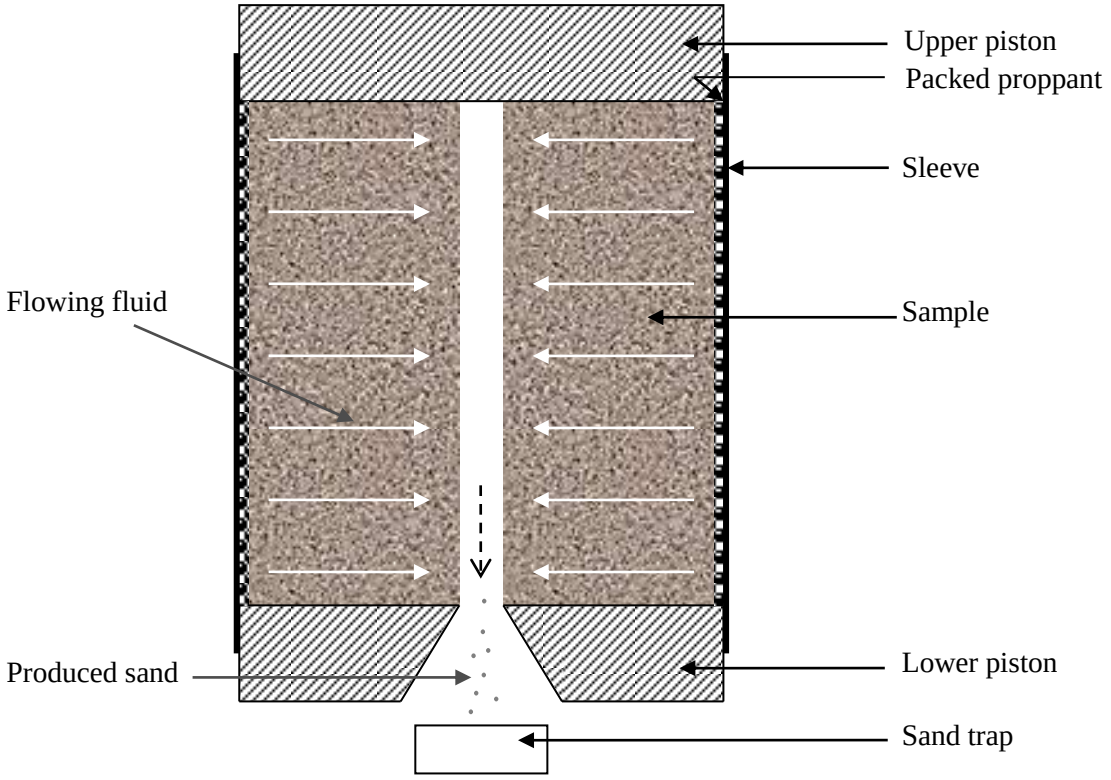

Figure 2 Schematic illustration of the sand production test setup

3.2 Synthetic sandstone

The first calibration test to be presented here is a test on a synthetic sandstone. This rock is created from sand cemented with sodium silicate, and has a porosity of about 26% and unconfined compressive strength of about 5 MPa. This material is classified as Class C according to Papamichos et al. (2008), and is characterised by grain point contacts, weak and porous cementation and bulging during failure in uniaxial compression. The test results are shown in Figure 3. The figure also shows the results of the model calculations, using the parameter set shown in Table 1. Equation (1), with the exception that $(D - D_c)/C_0$ is replaced with its original non-approximated expression, is used for these calculations (Equation (5)). Post failure analyses of the test sample show that the sand producing cavity has grown uniformly, thus maintaining its rotational symmetry in the process (Figure 1). This is one of the assumptions that Equation (1) is built on, as mentioned above.

Figure 3 shows that the model can be matched reasonably well to the test data. Note that the small bursts related to the discontinuous breakdown of the failed material under constant conditions have intentionally been smoothed out in the model, as their somewhat irregular nature cannot be modelled in detail anyway. Some small-scale discrepancy between the model and the observations is therefore to be expected. The increasing discrepancy between model and measurements towards the end of the test may be related to the high external stress and corresponding nonlinear effects which are not accounted for, either by Equation (1) or Equation (7). This discrepancy may also be related to boundary effects due to the interaction between the external boundary and the hole, especially with respect to fluid flow. This is only an experimental artefact since in reality there are no external boundary effects.

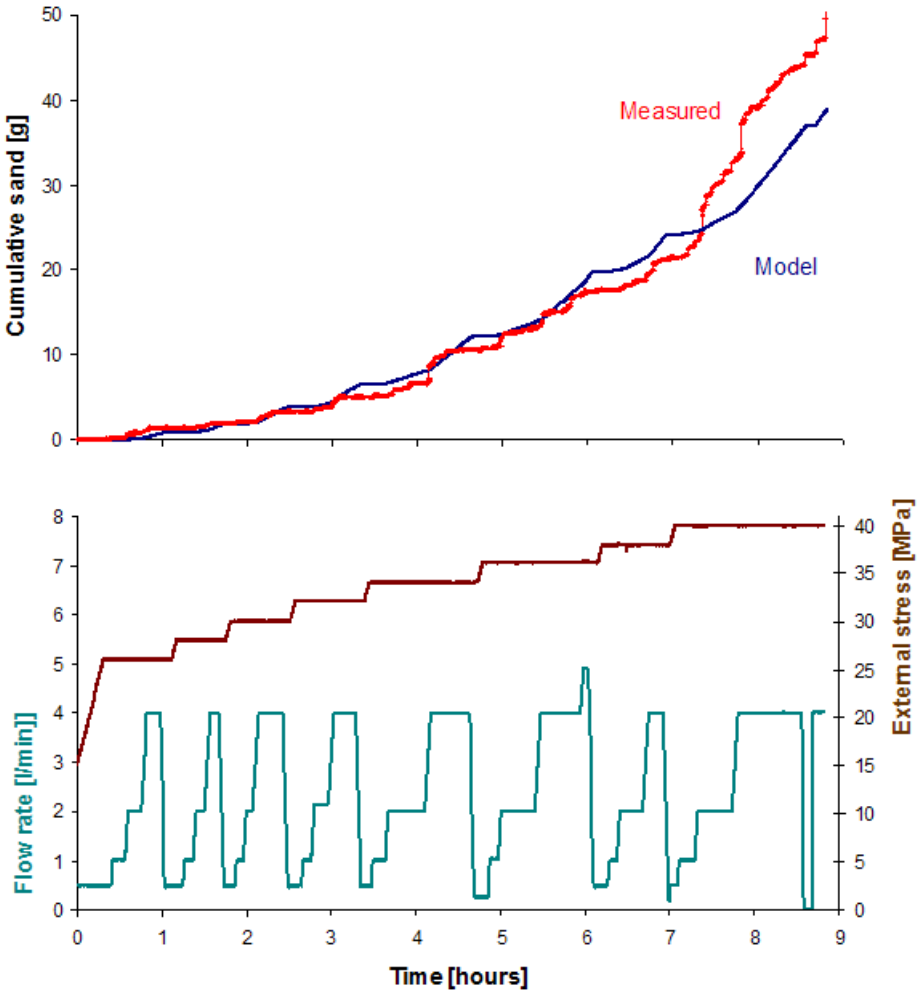

Figure 3 Sand production test results on synthetic sandstone

The set of parameter values given in Table 1 is not unique; as the parameters in the model are clearly coupled, there is significant uncertainty in the parameter values. The uncertainty ranges given in Table 1 are estimated standard deviations, based on the assumption that the number of independent observations is 500, which corresponds to about one per minute (whereas the number of recorded data points is about nine per minute). The number of independent observations is not well defined, as the amount of produced sand changes with time – according to the model as well as the observations – also during the periods of constant external conditions.

Table 1 Calibration data for sand production test on synthetic sandstone

Parameter	Calibrated Value	Uncertainty
τ_s	130 hours	77%
q_{fl}^{cr}	0.0003 m/s	44%
A_1	0.10	23%
A_2	4.0 MPa	15%

3.3 Red Wildmoor sandstone

The next calibration test was a test on Red Wildmoor sandstone. This is an outcrop rock with porosity of about 24% and unconfined compressive strength of about 12 MPa. This material is classified as Class B according to Papamichos et al. (2008), it has clay cementation and develops shear bands during failure in uniaxial compression.

The test results are shown in Figure 4. Post failure analyses of the test sample show that convex breakouts due to shear failure have developed during the test (Figure 1), hence only a part of the cavity surface has produced sand. Therefore, Equation (6) is used for the model calculations. The sand producing area is chosen to be $A_{sp} = A/2$. Due to the change in shape of the cavity during the test, the assumption that $Q_{sp}/A_{sp} \propto q_{fl}$ (fluid flux) – an underlying assumption in Equation (1) – may no longer hold. The relation:

$$\frac{Q_{sp}}{A_{sp}} = kp_e \tag{8}$$

is therefore used in order to estimate the flow rate. The proportionality constant k (= 0.002 m s^{-1} MPa^{-1}) is found by equating Akp_e to the measured flow rate Q at the initial part of the test. Both of these assumptions may be questioned, and in reality the relations may also change during the test.

A simple match of the model indicated that the measured sand production rate was relatively lower at the main part of the test than at the initial part when compared to the model predictions. This may have been caused by an increased stability of the cavity as the shape was changing, since the cylindrical shape may not be the most stable one for this type of rock – even under isotropic stress conditions. For the sand production model, this can be expressed as an increase in the critical drawdown as a function of the amount of produced sand. To account for this, we add an extra term:

$$\Delta D_c = A_3 \frac{\Delta m_{sand}^3}{A_4^3 + \Delta m_{sand}^3} \tag{9}$$

to Equation (7) for the critical drawdown. Δm_{sand} is the cumulative amount of sand per unit cavity length produced since the start of the test. Thus, we have a circular hole regime for $\Delta m_{sand} << A_4$, and an oval hole regime when $\Delta m_{sand} >> A_4$.

Figure 4 shows the results of the model calculations, using the parameter set listed in Table 2. As for the synthetic sandstone, the model matched the test data reasonably well. Again, the match is less convincing at the last part of the test, when the external stress is largest.

Also for this test the boundary effects due to the interaction between the external boundary and the hole may be of some significance at the later stages of the test. According to the model, the transition to oval hole occurs about five to six hours into the test.

The estimated standard deviations given in Table 2 are based on the assumption that the number of independent observations is 900, which corresponds to about one per minute (whereas the number of recorded data points is about nine per minute).

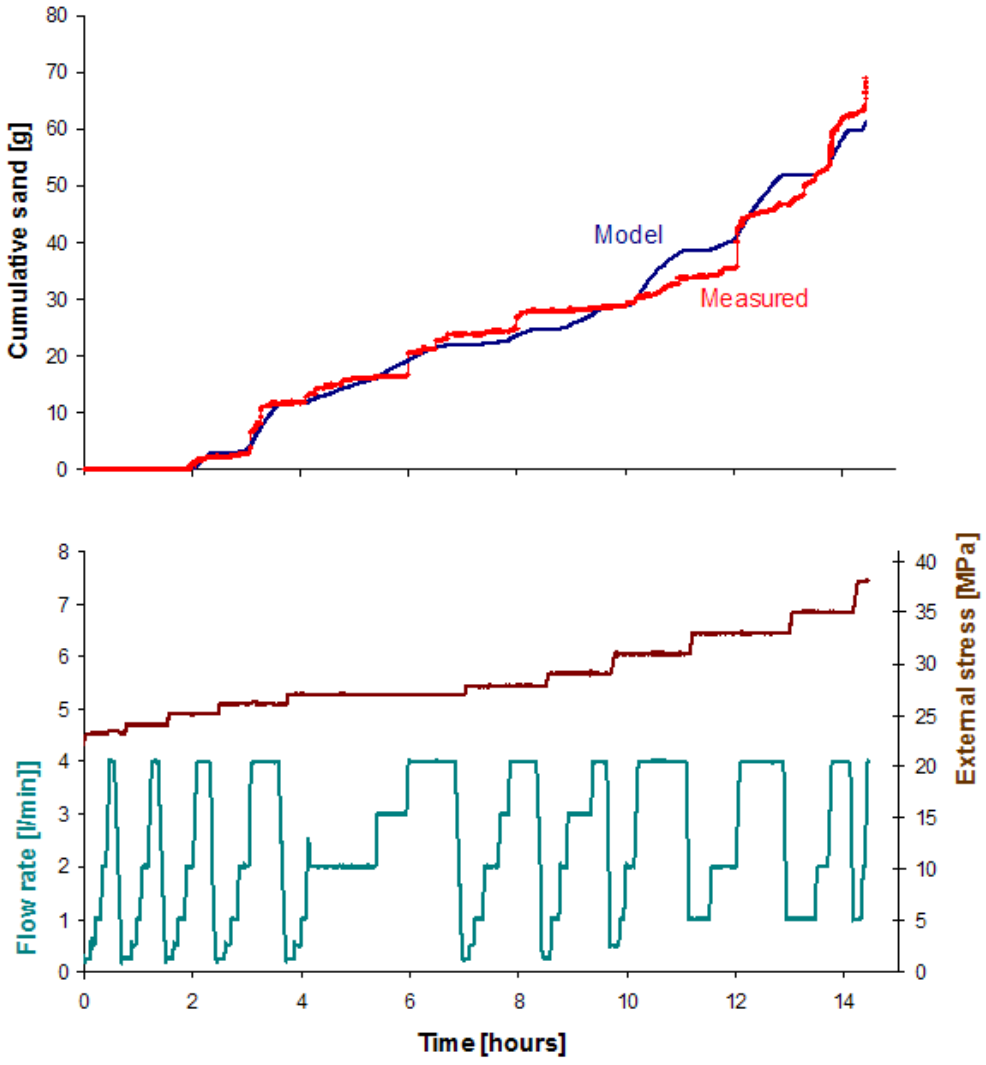

Figure 4 Sand production test results on Red Wildmoor sandstone

Table 2 Calibration data for sand production test on Red Wildmoor sandstone

Parameter	Calibrated Value	Uncertainty
τ_s	82.5 min	21%
q_{fl}^{cr}	0.0006 m/s	10%
A_1	0.25	< 1%
A_2	9.55 MPa	< 1%
A_3	4.36 MPa	10%
A_4	161 g/m	3%

3.4 Castlegate sandstone

Finally, we tried to analyse a test on Castlegate sandstone. This is an outcrop rock with porosity of about 24% and unconfined compressive strength of about 15 MPa. This material is classified as Class A according to Papamichos et al. (2008); it has quartz cementation, and fails by axial splitting in uniaxial compression. The test results are shown in Figure 5. In this test, very little sand is produced initially. However, at one point, where the external stress and the flow rate are constant (and the flow rate is quite low), the rate of sand production suddenly increased dramatically. Post failure analyses of the test sample show that the cavity had developed slit-like breakouts (Figure 1) that ran along the entire length of the sample, parallel to the cavity. The width of the slits appeared to be constant. Apart from a minor area at the slit entrance, the cavity appeared to be more or less undamaged. This failure mode – which is similar to the borehole failure mode described by Haimson and Kovacich (2003) – is clearly different from the ones observed in the previous tests.

To analyse this test, we use Equation (6). The sand producing area is assumed to be $A_{sp} = 2LW$, where W (= 3 mm) represents the width of the slits. As for the test on Red Wildmoor sandstone, the flow rate is estimated from the external pore pressure according to Equation (8), with $k = 0.004$ m s^{-1} MPa^{-1}. An initial attempt to apply this model showed that the observed sand production curve could be reproduced quite well, except that the onset of high rate sand production would have to occur earlier than observed. This indicates that the high rate process is preceded by a low rate process which creates the necessary conditions for the high rate process to initiate.

Table 3 Calibration data for sand production test on Castlegate sandstone

	Calibrated Value			
Parameter	Low Rate Process	Uncertainty	High Rate Process	Uncertainty
τ_s	139 hours	< 1%	0.142 s	4%
q_{fl}^{cr}	0.00015 m/s	< 1%	0.000217 m/s	< 1%
A_1	0.2	< 1%	0.2	< 1%
A_2	9.8 MPa	< 1%	11.65 MPa	< 1%
A_3	-		1.73 MPa	< 1%
A_4	-		15.5 g/m	3%

We attempted to capture this two step process, by using Equation (1) to model the low rate process, in addition to the high rate process modelled by Equation (6). We also subtract a term of the same form as Equation (9) from the critical drawdown used in Equation (6), in order to account for the reduced stability against the slit failure mode caused by the initial sand production. The parameters used are listed in Table 3. Figure 5 shows the results of the model calculations. We see that the model can match the test data reasonably well.

The estimated standard deviations given in Table 3 are based on the assumption that the number of independent observations is 160, which corresponds to about one per minute (whereas the number of recorded data points is about nine per minute). Clearly, the model is extremely sensitive to variations in the parameter values.

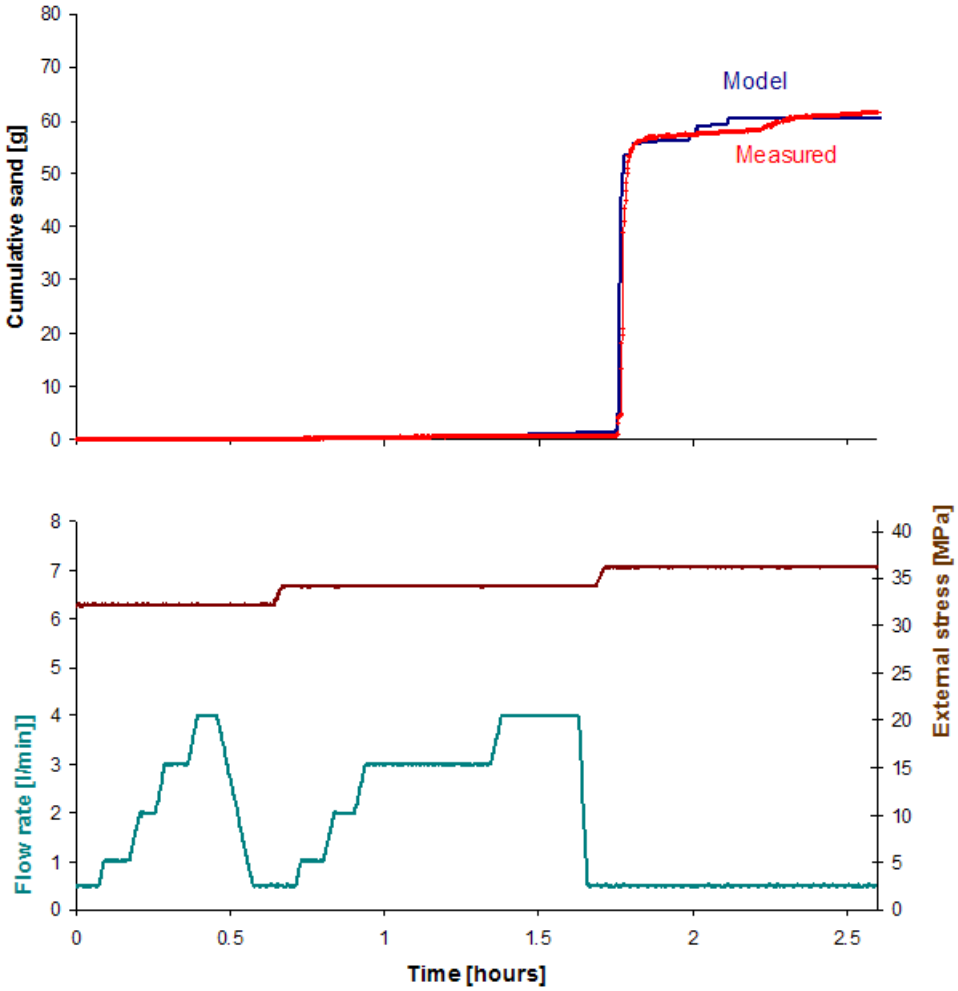

Figure 5 Sand production test on Castlegate sandstone

4 Predictions of the model

The model may now be used to make predictions for the rate of sand production, for various production scenarios. These predictions vary considerably, depending on the assumed in situ stresses and pore pressure, and on the production related parameters drawdown and pore pressure. Here we give a few examples, considering a single production cavity of length 0.5 m and diameter 2 cm which simulates a perforation cavity.

4.1 Step-change in drawdown

First, we considered a situation where the cavity was initially not producing any sand, but the production parameters were such that the cavity was at the onset of sand production. At time $t = 0$, the drawdown was increased by ΔD. Figure 6 shows how the sand cut develops with time, for three different values of ΔD, for the Class C (synthetic) sandstone. Note that the sand cut is defined as the mass of produced sand per unit volume of produced fluid. As expected, the cavity immediately starts to produce sand due to the increase in drawdown. We see that for a small increase in drawdown, the sand rate remains nearly constant for a long time, while for larger increases in drawdown, the sand rate peaks after a few days, then falls and eventually becomes lower than the rate found for the lower increase in ΔD.

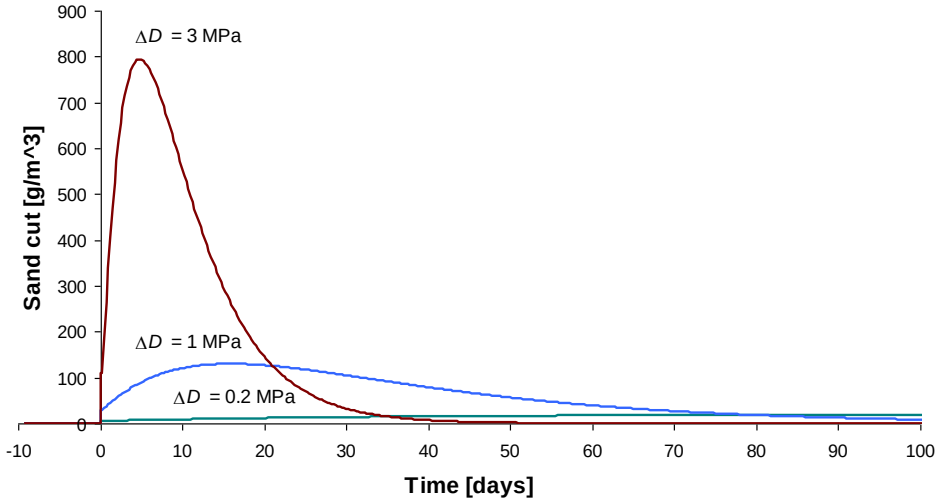

Figure 6 Comparison of predicted sand cut following an increase ΔD = 0.2, 1 or 3 MPa in drawdown, for the Class C (synthetic) sandstone

Figure 7 shows how the sand cut develops with time, for three different values of ΔD, for the Class B (Red Wildmoor) sandstone. For smaller increase in drawdown, the cavity will only produce a short burst of sand, and will quickly return to sand free production. According to the model, the cavity has attained a more stable shape after this transient event. As the inflow area has increased due to the removal of some sand, the flow rate has also increased as a result of this clean-up procedure. For the larger increase in drawdown, the cavity does not reach a stable state after the initial burst of sand has been produced, and will continue to produce sand. The model predictions are however somewhat uncertain for the long term development in this case.

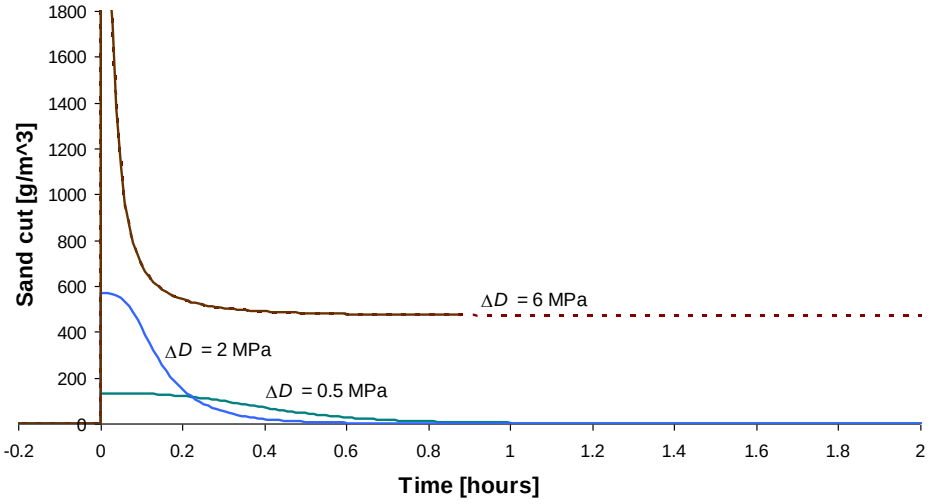

Figure 7 Comparison of predicted sand cut following an increase ΔD = 0.5, 2 or 6 MPa in drawdown, for the Class B (Red Wildmoor) sandstone

Figure 8 shows how the sand cut develops with time, for three different values of ΔD, for the Class A (Castlegate) sandstone. For the smallest increase in drawdown, the low rate sand production is initiated. However, the high rate production due to the formation of slit-like breakouts does not occur since the flow rate is not sufficiently high. For the larger increase in drawdown, the formation of slit-like breakouts is triggered after a while, leading to a very high rate of sand production. The subsequent drop in the sand cut is a result of the increased production due to the increase in inflow area: the sand rate in terms of mass per unit time remains at the high level. In practise, however, the process will be limited by flow restrictions – as

indicated on the curve for ΔD = 1.5 MPa. A complete sand-up of the well is a potential outcome of this situation.

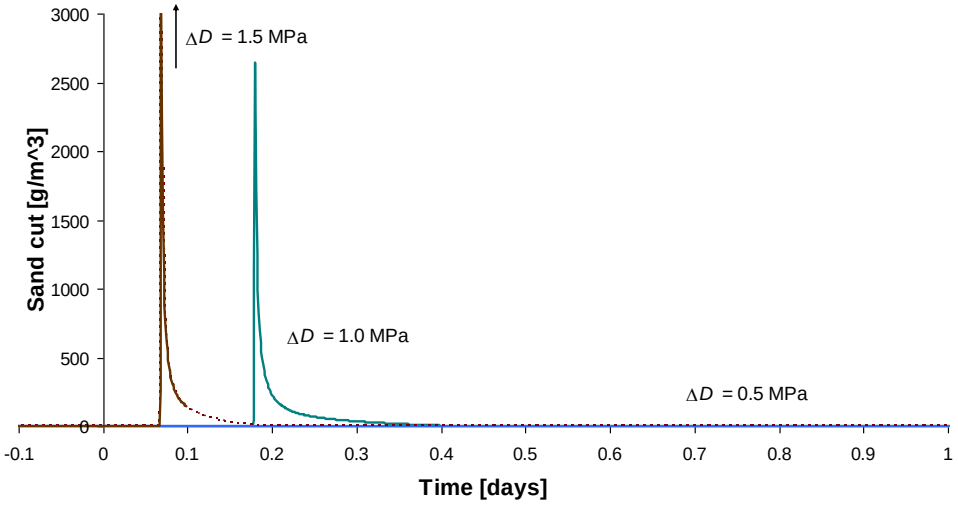

Figure 8 Comparison of predicted sand cut following an increase ΔD = 0.5, 1 or 1.5 MPa in drawdown, for the Class A (Castlegate) sandstone

4.2 Constant production, depleting reservoir

Next, we considered a situation where the cavity was maintained at constant flow rate production, while the reservoir was being depleted at a rate of 1 MPa per year. The cavity was initially producing sand free, but the increasing effective stresses due to the reduction in the reservoir pressure eventually triggered sand production. The onset of sand production is set to occur at t = 0.

Figure 9 shows how the sand cut, in terms of mass per unit volume of produced fluid, develops with time for the Class C (synthetic) sandstone. After the onset of sand production, the sand cut increases gradually as the reservoir depletion continues. However, the sand production leads to an increase in the inflow area, and the fluid flux (= flow rate per unit inflow area) is therefore reduced. Eventually, this reduces the sand cut and gradually terminates the sand production.

Figure 10 shows how the sand cut may vary with time for the Class B (Red Wildmoor) sandstone. At the onset of sand production, a small burst of sand will occur followed by a transient low rate production. This initial production changes the cavity into a more stable shape and the sand production gradually stops. Some time later, the increasing depletion eventually implies that the cavity is no longer stable even with its new shape, and sand production re-initiates – possibly at a much higher rate. The predictions are quite uncertain on this point, however, as the model is not calibrated for this situation.

Figure 11 shows how the sand cut may vary with time for the Class A (Castlegate) sandstone. The sand cut increases gradually after the onset of sand production, due to the low rate process. After about 110 days, the formation of slit-like breakouts is initiated. In this case, the assumption of constant flow rate implies that the creation of the slit-like breakouts is only slowly progressing, since the well pressure is constantly adjusted as the inflow area is increasing. In practise, the development may be quite different, depending on the response times of the well and the production equipment. Since the formation of these breakouts is a very fast process under constant drawdown conditions, it is a risk that they may have time to produce a lot of sand before the flow rate is restabilised. The predictions may therefore vary considerably, depending on the assumed conditions.

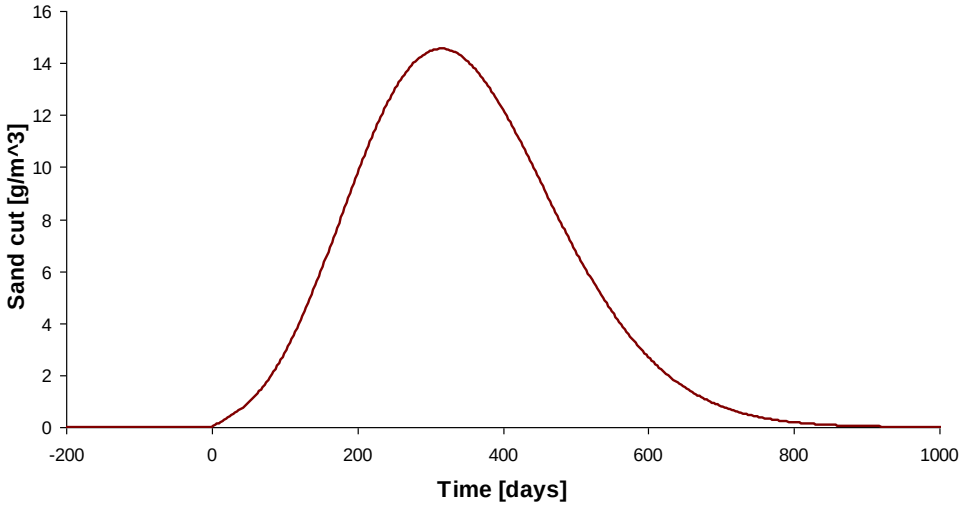

Figure 9 Predicted sand cut versus time for a cavity in a depleting reservoir, for the Class C (synthetic) sandstone

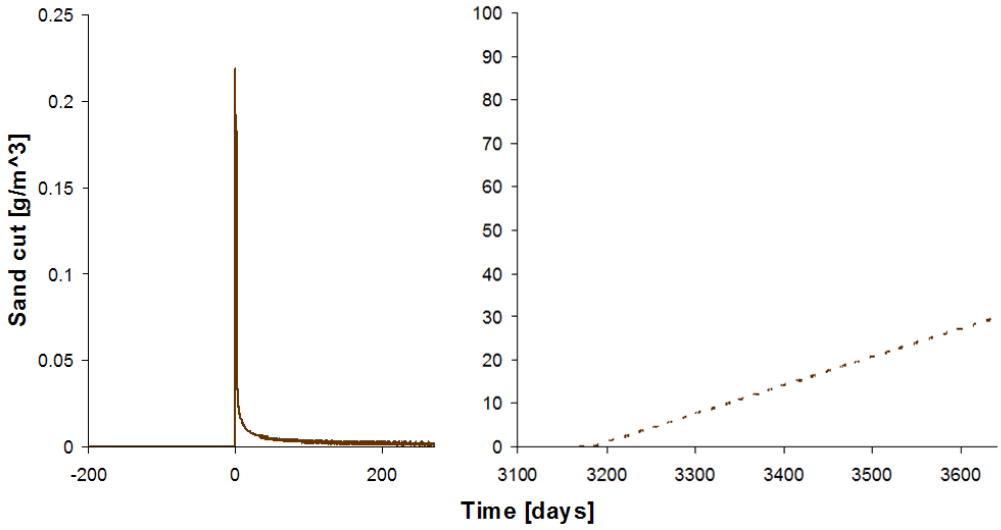

Figure 10 Predicted sand cut versus time for a cavity in a depleting reservoir, for the Class B (Red Wildmoor) sandstone

5 Discussion

The calibration tests show that there are clear differences between the three different rock classes with respect to sand production from these rocks. Although there is significant uncertainty related to the calibration of the model, some trends are still quite clear. When comparing the calibrated parameters, we notice a major difference between the rock types with respect to the characteristic sand erosion time, which differs by orders of magnitude. Also the changes in the critical drawdown induced by the sand erosion process itself differ significantly, as D_c decreases (initially) with time for the Class A rock, it increases with time for the Class B rock, and it remains unaffected for the Class C rock. On the other hand, the critical fluid flux does not differ very much between the classes.

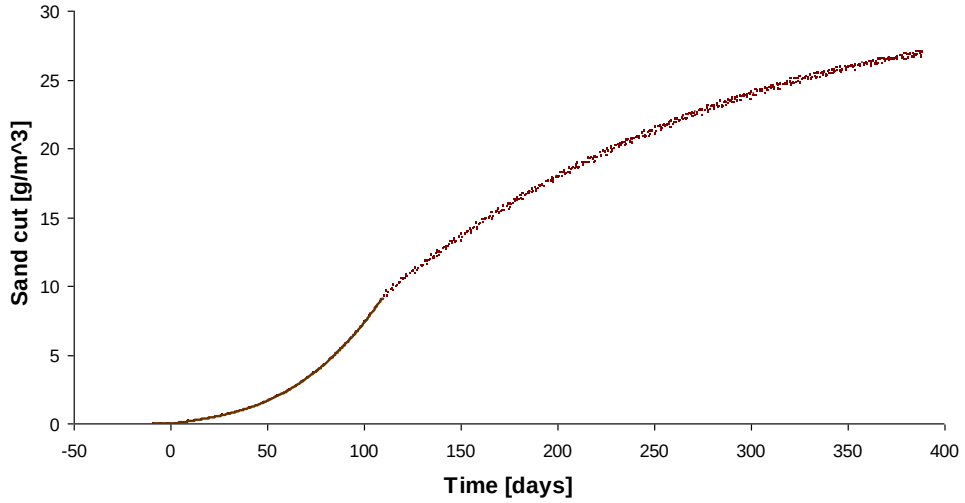

Figure 11 Predicted sand cut versus time for a cavity in a depleting reservoir, for the Class A (Castlegate) sandstone

Some important aspects of the problem have not been included in the model. For instance, the possibility that mobilised sand is clogging the cavity entrance, thus forming a stable sand arch, a situation which may allow for more or less sand free production, even under conditions far beyond the onset of sand production according to this model. Other developments which are not accounted for by the model, include the possible collapse of the slit-like breakouts when they reach a critical size.

The fluid viscosity is known to have an impact on the sand production rate. This relation was not studied here, and the effect is not explicitly shown in the equations above. However, it can be shown (Fjær et al., 2008) that the characteristic sand erosion time τ_s is inversely proportional to the fluid viscosity.

6 Conclusions

We have shown that a simple analytical model for the rate of sand production may be calibrated on data from laboratory tests where sand production from cylindrical cavities is simulated. The calibrated model may then be used to simulate sand production under field-like conditions.

Some modifications of the model were needed in order to obtain a reasonable match with the laboratory data. In particular, we have introduced the possibility for a change in critical drawdown induced by the sand erosion process itself. The nature of this feature varied between the three different rock types analysed in this study.

When applied to simulate field-like conditions, the model illustrates that the sand rate may vary very slowly in some cases, thus making it appear as constant. In other cases, the sand production will appear as a time limited event, typically initiated with a burst followed by a tail of slowly decaying sand rate. In some cases, the sand rate may be so high that the situation could be catastrophic. It is seen that the predictions vary considerably with rock type, in situ stress and pore pressure conditions, and the production related parameters drawdown and flow rate.

Acknowledgements

The authors would like to acknowledge the past and current support of the partners of The Foundation for Scientific and Industrial Research (SINTEF) Petroleum Research JIP in “Volumetric sand production”, Chevron, ConocoPhillips, Eni, Hess, Petrobras, StatoilHydro, Total, Shell.

References

Fjær, E., Cerasi, P., Li, L. and Papamichos, E. (2004) Modeling the Rate of Sand Production. ARMA/NARMS 04-589. Gulf Rocks 2004.

Fjær, E., Holt, R.M., Horsrud, P., Raaen, A.M. and Risnes, R. (2008) Petroleum Related Rock Mechanics. 2nd Edition. Elsevier, Amsterdam 491 p.

Haimson, B. and Kovacich, J. (2003) Borehole instability in high-porosity Berea sandstone and factors affecting dimensions and shape of fracture-like breakouts. Engineering Geology 69, pp. 219–231.

Hettema, M., Andrews, J., Blaasmo, M. and Papamichos, E. (2006) The relative importance of drawdown and depletion in sanding wells: Predictive models compared with data from the Statfjord field. 2006 SPE International Symposium and Exhibition on Formation Damage Control, Lafayette, Los Angeles, USA.

Papamichos, E., Vardoulakis, I., Tronvoll, J. and Skjærstein, A. (2001) Volumetric sand production model and experiment. Int. J. Numer. Anal. Methods Geomech. 25(8), pp. 789–808.

Papamichos, E., Stenebråten, J., Cerasi, P., Lavrov, A., Vardoulakis, I., Fuh, G-F., Goncalves, C.J. de C. and Havmøller, O. (2008) Rock type and hole failure pattern effects on sand production. ARMA 08-217. 42nd US Rock Mechanics Symposium and 2nd Canada–U.S. Rock Mechanics Symposium, San Francisco, June–July, 2008.